Energetics and kinetics of CO and NO adsorption on Pt{100}: Restructuring and lateral interactions

Y. Y. Yeo, L. Vattuone, and D. A. King
Department of Chemistry, University of Cambridge, Lensfield Road, Cambridge, CB2 1EW, United Kingdom

(Received 2 August 1995; accepted 31 October 1995)

Calorimetric heats of adsorption and sticking probabilities are reported for NO and CO on both the reconstructed hex and the unreconstructed (1×1) surfaces of Pt{100} by single crystal adsorption calorimetry (SCAC), at room temperature. The hex surface reverts to the (1×1) structure during adsorption of both gases, as previously reported. The initial heat of adsorption on the (1×1) surface is 215 kJ/mol for CO and 200 kJ/mol for NO. Adsorbate–adsorbate interactions determine not only the dependence of the heat of adsorption on coverage but also the formation of different ordered structures. A model is suggested to explain the observed dependence of the differential heat on coverage and the LEED patterns, and a Monte Carlo simulation is performed to derive the corresponding differential heat, thus allowing estimates to be made of the magnitude of adsorbate–adsorbate interactions. For CO adsorption, the critical contribution is the pairwise interaction energy ϵ_d between molecules in *nnn* sites while for NO triplet formation is suggested with significant repulsive interaction between molecules in the same triplet (ϵ_t) and an even stronger repulsion between triplet pairs (ϵ_{tt}). NO–NO repulsive interactions (ϵ_t=20 kJ/mol, ϵ_{tt}=80 kJ/mol) are considerably stronger than CO–CO interactions (ϵ_d=5 kJ/mol); thus, at half monolayer coverage CO gives rise to a $c(2\times2)$ pattern while NO gives a $c(2\times4)$ pattern. Moreover, with CO the coverage can be increased to 0.75 ML, with the formation of compressed structures, while for NO the saturation coverage is just 0.5 ML. The differential heat on the hex surface is also discussed showing the possible role of adsorption at defect sites in the energetics of the system. The surface energy difference between the clean (1×1) and hex surfaces is obtained as 20 kJ(mol Pt_s)$^{-1}$ by comparing the integral heats of adsorption of CO on both surfaces at θ=0.5, when the final states of the two systems are identical. © *1996 American Institute of Physics.* [S0021-9606(96)01006-X]

I. INTRODUCTION

Considerable attention has been given to the adsorption and reactions of CO and NO on Pt{100}, in relation to both an adsorbate-induced surface phase transition and the catalytic reaction of these two adsorbates to CO_2 and N_2. This is the first detailed study of the calorimetry of these two systems, providing important information relevant to energy pathways and lateral interactions between adsorbed species.

The adsorption of NO on Pt{100} has been investigated by LEED,[1] TDS,[2] RAIRS,[3] EELS,[4] STM,[5] molecular beams,[6,7] FEM,[8] and other techniques, particularly in relation to the oscillatory NO+CO reaction.[9] Similar investigations have also been carried out for CO,[10,11] and recently an extensive investigation of CO adsorption has been performed using molecular beams.[12] However, the heat of adsorption has never been measured directly on this single crystal surface but only inferred through the analysis of thermal desorption curves[2] or from isosteres obtained using LEED.[13]

The clean Pt{100} surface is reconstructed at room temperature with the topmost layer showing either a hex or a hex-*R* structure[14] depending on the annealing temperature reached during the preparation. A metastable unreconstructed (1×1) surface can also be prepared by standard procedures.[14,15] Adsorption of gases such as ethylene,[5] CO,[12] NO,[14] H_2 and O_2[15] drives a phase transition from the initial hex (or hex-*R*) phase to the (1×1) phase. A nonlinear growth law for this phase transition[12] has been demonstrated to be a key factor in explaining the oscillatory kinetics observed on this surface at 480–500 K for the NO+CO reaction[9] and for the CO+O_2 reaction.[16] Over the total CO coverage range from 0.03 to 0.5 ML Hopkinson and King[9] found that the local coverage on the growing (1×1) phase islands ranges between 0.44 and 0.47 ML, depending on CO pressure (or beam flux), while the local coverage on the remaining hex phase areas is always very low, in the range 0.01 to 0.03, depending on pressure.[12]

In a brief report from the present work, the surface energy difference between the clean hex and (1×1) phases has been derived as 20 kJ (mol Pt_s)$^{-1}$ by comparing the integral heat of adsorption of CO on Pt{100} (1×1) with that on the hex surface at half a monolayer coverage when both the hex and (1×1) phases have been converted to a Pt{100}–CO–$c(2\times2)$ phase.[17]

Adsorption of CO on the (1×1) phase leads to the formation of a $c(2\times2)$ superstructure;[10] the half order beams appear as fuzzy spots which sharpen and intensify with increasing coverage, their intensity starts to rise significantly at a coverage of 0.2 to 0.3 ML and reaches its maximum at 0.5 ML, as expected for an ideal $c(2\times2)$ structure. At higher coverages, the intensity of half order beams drops very rapidly and spots broaden, indicating a loss of order in the overlayer.[10] On the hex surface the beams corresponding to the hex structure gradually fade with increasing coverage and disappear completely at 0.5 ML; at the same time the (1/

 0021-9606/96/104(10)/3810/12/$10.00

2,1/2) beam, indicative of the $c(2\times2)$ structure, is already appreciable at 0.1 ML and increases in intensity, reaching its maximum at 0.5 ML. Further exposure gives rise to high coverage structures: first a $c(5\sqrt{2}\times\sqrt{2})$ [corresponding to a coverage of 0.6 ML (Ref. 11)], then a $(3\sqrt{2}\times\sqrt{2})$R45° structure (corresponding to a coverage $\theta_{CO}=0.67$) and finally, at saturation ($\theta_{CO}=0.75$), a $c(2\times4)$ structure together with a $(3\sqrt{2}\times\sqrt{2})$R45° pattern.[10]

Martin *et al.*[11] investigated this system by RAIRS and report a single linear band on the (1×1) surface at 300 K, shifting from 2065 to 2090 cm^{-1} with increasing coverage and at least three different bands in the bridge region at frequencies between 1867 and 1910 cm^{-1}, depending on coverage. The ratio of bridge to linear intensity attains its maximum around 0.5 ML, in agreement with a previous HREELS study.[10] On the hex surface more complex behavior was observed: at low exposures a feature at 2083 cm^{-1} is observed and assigned to CO adsorbed in a linear configuration on the hex surface without restructuring; at a coverage of about 0.13 ML it is believed that conversion to the (1×1) structure is signaled by the appearance of a linear band at about 2089 cm^{-1} accompanied by the appearance of a band at 1873 cm^{-1}, assigned to bridge sites. The assignment of the feature at 2083 cm^{-1} to adsorption on the unrestructured hex surface is subject to question, because it is at variance with the conclusion by Hopkinson *et al.*, who reported that the hex to (1×1) structure conversion starts at a much lower coverage, 0.01 to 0.03 at 400 K, depending on flux, and that the conversion rate is temperature invariant above 200 K.[6,12] As we shall show, our measurements support the thesis of Hopkinson *et al.* and a different assignment for that band is suggested. With increasing coverage, the linear band shifts to 2098 cm^{-1}; the small frequency shift compared to that observed on the (1×1) surface is due to the relatively small change in *local* coverage with increasing total coverage.

The behavior of NO is more complicated than that of CO. Due to its amphoteric character NO exhibits a wide range of vibrational frequencies in its different compounds. It is reported to adsorb nondissociatively on the hex phase at room temperature and molecularly with a small degree of dissociation on the (1×1) phase.[4,18]

Adsorption of NO on the hex surface gives rise to two IR bands, one at 1628 cm^{-1}, shifting to 1638 cm^{-1}, which is attributed to NO adsorbed in a bent configuration at a position intermediate between on top and bridge sites and the other shifting from 1789 to 1805 cm^{-1} assigned to NO adsorption at defect sites.[3,4] From the early stages of the adsorption sequence the LEED pattern shows superposition of the clean hex and the $c(2\times4)$ overlayer. At saturation coverage ($\theta_{NO}=0.5$) the beams corresponding to the hex structure are quenched. As for CO, an island formation mechanism is suggested with high local coverage within the islands, thus explaining both the small frequency shift and the early appearance of the $c(2\times4)$ beams. Adsorption on the (1×1) surface gives rise to only one band, at 1596 cm^{-1}, which shifts to 1641 cm^{-1} at saturation. A very faint feature at 1800 cm^{-1} is observed at very high coverage. The $c(2\times4)$ pattern appears only at coverages close to saturation. No lower coverage pattern has been reported; in particular a $c(2\times2)$ pattern is not observed. The sticking probability has not been investigated as extensively as for CO, but similarly high values of the initial sticking probability have been inferred.[14]

There are interesting similarities between NO and CO adsorption: both adsorb with high initial sticking probabilities; both drive the reconstruction of the clean hex surface; and in both cases the adsorption is almost entirely nondissociative. But there are also remarkable differences, in saturation coverages, in ordered structures and in adsorption sites. A comparison of NO and CO on Pt{100} is thus a fruitful area for investigation.

Single crystal adsorption calorimetry (SCAC) provides a direct means of measuring heats of adsorption as a function of coverage for irreversible as well as reversible adsorption.[19,20] In this paper we report adsorption heats and sticking probabilities for NO and CO on Pt{100} at room temperature.

II. EXPERIMENT

The instrument for SCAC is described in detail elsewhere.[19,20] Briefly, NO or CO molecules supplied by a pulsed supersonic nozzle source at room temperature, are adsorbed on a 200 nm thick Pt single crystal film supported on a Pt ring. The pulses are 50 ms long at a beam flux $Q\sim2\times10^{13}$ mol cm^{-2} s^{-1} and are separated by a 2.5 s time interval. Changes in infrared emission due to the increased temperature during adsorption are detected by a Hg–Cd–Te infrared detector. The peak-to-peak signal is directly proportional to the heat released to the sample by the impinging molecules. The intensity is calibrated by comparison with the infrared emission observed when a chopped laser beam of known power and with the same temporal and spatial structure as the molecular beam strikes the crystal at normal incidence. The power of the laser is measured by a calibrated photodiode. Measurements are repeated six or seven times and then averaged to reduce the standard deviation of the final differential heat; sticking probabilities are measured by the King and Wells reflection detector technique[21] and the absolute intensity of the beam needed for coverage calibration is obtained by a spinning rotor gauge; the coverage is obtained by summing up the amount of gas adsorbed from each pulse. As more gas is dosed onto each surface, a steady state is eventually attained when the amount of NO (or CO) added during each 50 ms pulse is exactly balanced by the quantity which desorbs between pulses. Once significant desorption occurs, summing the contributions thus gives rise to an ''apparent coverage'' scale which extends indefinitely while the true coverage reaches a limit, determined by the pulse intensity and the temperature.

The uncertainty in the coverage is mainly determined by the uncertainty in the sticking probability. At low coverage where the sticking probability is high the standard deviation in the coverage over seven different measurements is lower than 0.005 ML, and increases with increasing coverage up to about 0.03 ML. The uncertainty in the sticking probability also affects that in the heat of adsorption. The intensities

recorded by the detector at each pulse are averaged together to achieve the required signal-to-noise ratio. At low coverage where both the sticking probability and the heat of adsorption are high many points may be obtained with a good coverage resolution, while at high coverage the number of pulses needed to be averaged together to reach the desired sensibility is larger, thus making the coverage resolution poorer. Since the signal-to-noise ratio is fixed, the absolute errors on the heat of adsorption, given by the standard deviation on several measurements, is comparable at different coverages but the relative errors are much larger at high coverage, as expected. The details of the analysis procedure have been extensively discussed elsewhere.[19,20]

The hex surface was cleaned by mild argon ion sputtering and annealing. The (1×1) surface was obtained by adsorption of oxygen on a sputtered and unannealed surface at room temperature followed by annealing and hydrogen clean-off reaction. This procedure is somewhat unconventional but unavoidable to obtain a (1×1) surface in our experimental layout, since the usual method involving adsorption of oxygen at 580 K followed by reduction in H_2[14,15] is impracticable in our apparatus due to difficulties in monitoring the temperature of the crystal during heating. The cleanliness of the sample was checked by Auger spectroscopy. The main contaminant was *C*: sputtering and annealing cycles are repeated until the corresponding feature in the Auger spectrum disappears. The symmetry and crystallinity of the surface were monitored by LEED.

Rather importantly for what follows, the maximum annealing temperature is approximately 600 K, i.e., lower than usual for similar experiments on the same system.[6,7,14] Higher temperatures could not be used because of the need to avoid diffusion into the bulk of the amorphous carbon layer deposited on the back face of the crystal. This layer is used to increase the emissivity of the back face of the film. Care must therefore be used in comparing our sticking probability data with other work where the annealing temperature was higher. This directly affects both the degree of order of the surface, as already suggested by Thiel *et al.*[13] and proved by STM,[5] and the activity of the surface, as proved in a recent investigation of the hydrogen–deuterium catalytic exchange reaction on Pt{100}.[7] The procedure employed in the present work to prepare the (1×1) surface may produce a lower degree of order. This is not expected to modify substantially a local property such as the heat of adsorption but may strongly influence the coverage dependence of the sticking probability in precursor-mediated adsorption, where the number of possible steps may be altered if the order is incomplete.

Finally we note that the temperature rise is measured over a 100 ms period; only those processes which take place within this time scale are reflected in the heat measurement. The measured enthalpy change ΔH is always negative for adsorption. We therefore follow convention in defining the positive quantity $q=-\Delta H$ as the differential heat of adsorption.

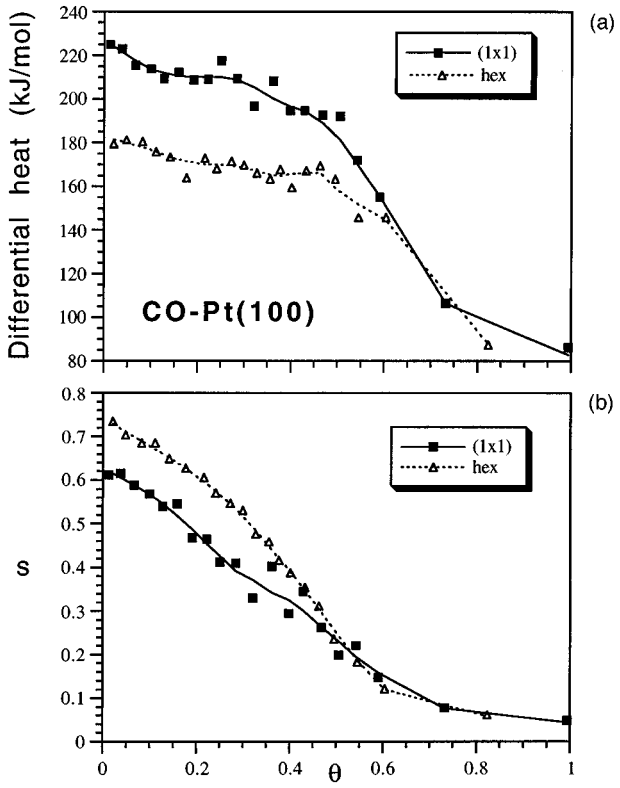

FIG. 1. (a) Differential heat of adsorption [in kJ/(mol CO)] for CO on Pt{100} as a function of coverage θ for the initially hex surface and for the (1×1) surface at 300 K. In this and in the following figures, the coverage θ is "apparent" as explained in the text and is expressed relative to a monolayer of Pt atoms on the Pt{100}–(1×1) surface; at coverages <0.7 ML θ is the true coverage. (b) The sticking probability *s* as a function of coverage for CO adsorption on the (1×1) and hex surfaces of Pt{100}. Dosing is performed by a supersonic molecular beam of high purity CO with the nozzle at room temperature and the molecules impinging on the surface at normal incidence.

III. RESULTS

A. CO adsorption

Figure 1 (upper part) shows the differential adsorption heat dependencies on coverage for CO on Pt{100} (1×1) and on Pt{100} hex, at room temperature. The differential heat for the (1×1) surface is initially 225 kJ/mol. After an initial decrease it remains constant at ~215 kJ/mol between 0.05 and ~0.25 ML, before falling to a second plateau at ~195 kJ/mol between ~0.25 and ~0.5 ML; thereafter it decreases abruptly until it reaches a steady-state average value of ~85 kJ/mol. The differential heat for the hex surface behaves differently. It is initially ~180 kJ/mol and decreases gently to a plateau at 170 kJ/mol between 0.15 and 0.5 ML before decreasing abruptly to the same value observed for the (1×1) surface, while approaching steady state. In the lower part, the sticking probability, *s*, is shown for both (1×1) and hex initial states of the Pt{100} surface. For the hex surface *s* is initially 0.73, decreasing almost linearly to 0.26 at $\theta\sim0.5$, then approaching slowly the steady-state value (0.04). A small deviation from linearity is observed at intermediate coverage (0.1–0.4 ML), in agreement with previously pub-

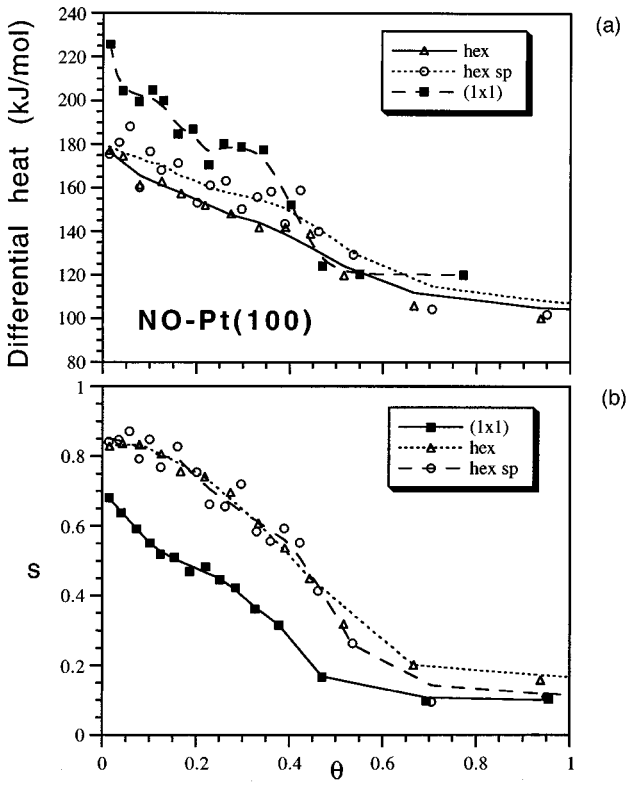

FIG. 2. (a) Differential heat of adsorption for NO on Pt{100} as a function of coverage θ for three different initial states of the surface: (1×1), hex and hex sputtered (hex *sp*). At coverages <0.5 ML, θ is the true coverage. (b) Sticking probability for NO on Pt{100} as a function of coverage for the three initial states of the upper part.

lished data.[10,12] On the (1×1) phase the sticking probability decreases almost linearly up to $\theta \sim 0.5$; from this point on it takes the same values as for the initial hex surface.

B. NO adsorption

The surface coverage dependence of the adsorption heat for NO on Pt{100} in three different initial states, hex, (1×1) and a sputtered and unannealed hex surface (labeled "hex *sp*") are shown in Fig. 2 (upper part). The sputtered surface was produced by argon ion sputtering an annealed hex surface for 10 min at a discharge current of 10 mA, corresponding to 2 μA/cm^2. The coverage is absolute until desorption becomes appreciable on a 2.5 s time scale, approaching $\theta_{NO}=0.5$, the true saturation coverage.[3] The differential heat for the annealed initially hex surface decreases almost monotonically from the initial value, ~177 kJ/mol, to 139 kJ/mol at $\theta=0.44$ and then reaches the steady-state value (~110 kJ/mol) more abruptly. The differential heat for the sputtered hex surface follows a similar trend, with a slightly higher initial value and decreasing up to saturation, remaining always a bit higher than for the hex surface. The (1×1) surface behaves differently: The heat is initially higher (about 225 kJ/mol), and is then practically constant in the range 0.05–0.12 ML; at 0.12 ML a small decrease is observed and the heat remains again roughly constant up to 0.35 ML, before a sudden decrease takes place; at saturation its value is the same as for the hex surface (110 kJ/mol), within experimental error.

Figure 2 (lower part) shows the sticking probability *s* as function of coverage for the same three initial states of the Pt{100} surface. For the hex and hex sputtered surface *s* is the same within experimental error: The zero coverage sticking probability is 0.82 and decreases to 0.13 at steady state. On the (1×1) surface it is initially lower (0.68) and decreases almost linearly up to steady state, where its value is the same as for the hex surface. A slight plateau is present at around 0.2 ML. At saturation coverage (0.5 ML) the sticking probabilities on hex and (1×1) surfaces do not coincide exactly, the value for the (1×1) being slightly lower, thus suggesting that the actual state of the surface at that point is not *exactly* the same. The hex reconstruction may be incompletely lifted to the (1×1) structure by NO adsorption.

IV. DISCUSSION

A. CO adsorption

Two different coverage ranges may be identified: The first (0 to 0.5 ML) is characterized by a smooth variation of the heat of adsorption with coverage while in the second (0.5 to 0.75 ML) a rapid drop is observed. The behavior of the (1×1) surface and of the initially hex surface are different in the first range but identical in the second. As may be inferred from the spectroscopic data reviewed in the introduction, two different adsorption sites are found and identified as atop and bridge sites.

In the 0 to 0.5 ML coverage range, CO adsorption takes place randomly on the (1×1) surface while on the initially hex surface it drives the reconstruction and islands of (1×1) character form with high local CO coverage. At a coverage of 0.5 ML the surface is completely converted to (1×1), and both surfaces attain the same final state, as proved by LEED and spectroscopic investigations; moreover, at this point our measured curves for both the differential heat and the sticking probability (Fig. 1) on the (1×1) and initially hex surfaces match, thus further supporting this conclusion. This process is shown schematically in Fig. 3. In the 0.5 to 0.75 ML range high coverage compressed structures [$c(5\sqrt{2}\times\sqrt{2})$, $(3\sqrt{2}\times\sqrt{2})$ and $c(2\times4)$] form for both initial states.

Since during the adsorption no work is done, the total heat released is identical to the change in the energy of the system. The same final state [Pt{100}(1×1)c(2×2)-CO], corresponding to a coverage of 0.5 ML, is reached starting from both the clean (1×1) [path (a) in Fig. 3] and the clean hex surfaces [path (b), again in Fig. 3]. The difference between the heats released during these two paths is just the energy difference between the two initial states [clean (1×1) and clean hex surfaces]. This difference is easily expressed in terms of the integral heat, defined as follows:

$$q_{\text{int}} = \int q_{\text{diff}}\, d\theta/\theta. \tag{1}$$

The integral heat for CO adsorption on the hex and (1×1) surfaces is shown in Fig. 4 (lower part). The difference be-

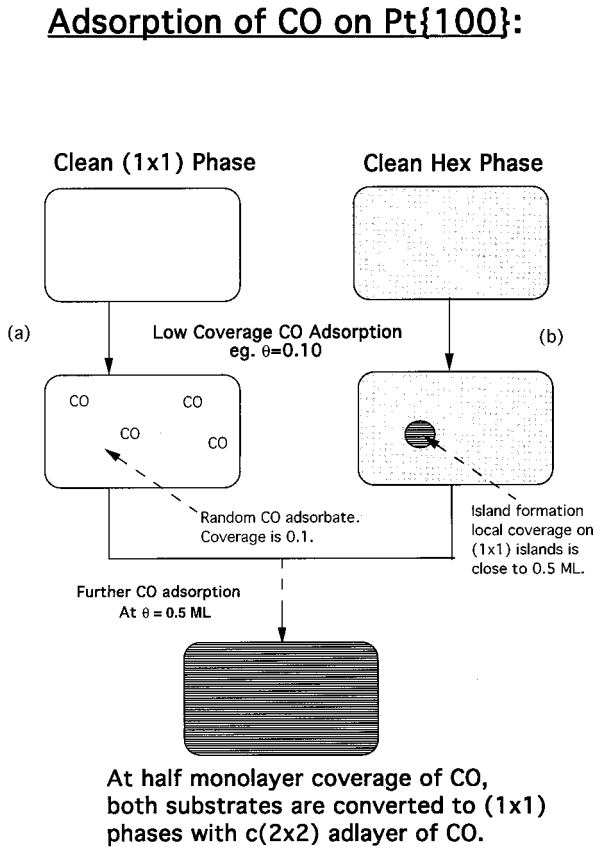

FIG. 3. Schematic diagram showing the two initial states of Pt{100} clean (1×1) and clean hex, and different CO adsorption pathways, (a) and (b), with island formation along (b) and the identical final state, Pt{100}(1×1)-$c(2\times2)$-CO. The difference in the integral adsorption heat along paths (a) and (b) is just the energy difference between the initial states.

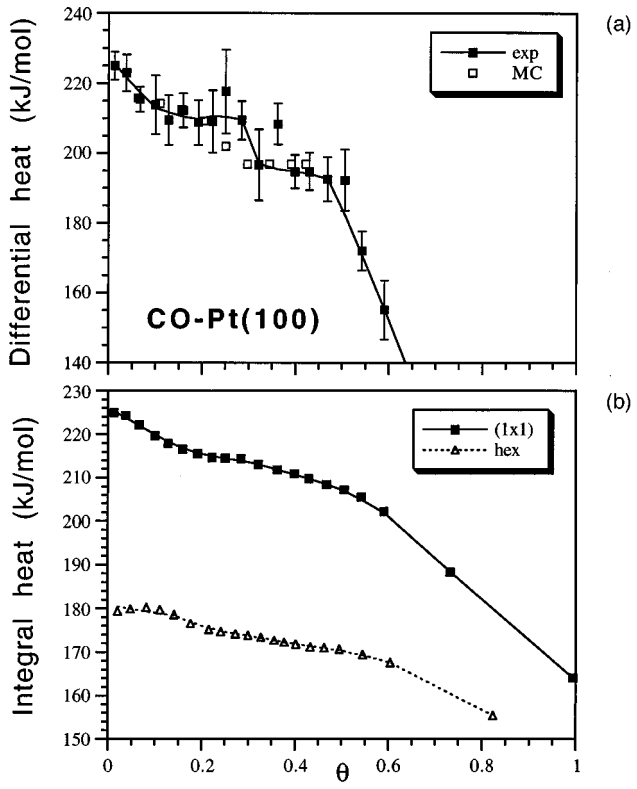

FIG. 4. (a) A comparison between experimental (exp) and simulated Monte Carlo (MC) values for the coverage dependence of the differential heat of adsorption of CO on the Pt{100}(1×1) surface. The error bars for the experimental data are also shown. (b) Integral heats [Eq. (1)] for CO adsorption on Pt{100}(1×1) and Pt{100}hex as a function of coverage.

tween the integral heats for adsorption on the (1×1) and hex surfaces, taken at 0.5 ML coverage multiplied by the coverage (0.5) is just the energy difference q_{spt} corresponding to the surface phase transition (spt) between the two clean surface phases of Pt{100} expressed in terms of the number density of surface Pt atoms, Pt_s. As previously reported,[17] $q_{\mathrm{spt}}=(20\pm2)\mathrm{kJ\ (mol\ Pt}_s)^{-1}$.

On the (1×1) surface there is a sharp fall in q_{diff} at low coverages. This may be attributed to adsorption at defect sites; the fall ends at 0.05 ML, and it seems reasonable to identify these defects as steps separating terraces whose length is about 20 atomic spacings. Subsequently q_{diff} is constant, between 0.05 and 0.25 ML, implying that there are no substantial repulsive interactions between adsorbed molecules up to that coverage. However the subsequent fall in q_{diff} in the range from 0.25 to 0.5 ML indicates that mutual repulsions between molecules are invoked. Lateral interactions between molecules may arise from three contributions: dipole–dipole interaction, Pauli repulsion (both through-space) and substrate-mediated (through-bond).[22] The contribution from dipole–dipole coupling is small;[23] and Pauli repulsion, accounting for the overlap of filled orbital electron wave functions, is important at short spacings. Substrate-mediated interactions are the main contribution at intermediate spacings; these interactions depend on the spacing and on the symmetry direction, and may be attractive or repulsive. In order to extract the magnitude of lateral interactions we have performed Monte Carlo simulations of CO adsorption by using a square lattice of sites. The following approximations are made.

(1) The heat of adsorption is assumed to be the same for bridge and atop sites. This assumption is supported by the fact that on the (1×1) surface both sites are occupied at low coverage so that no sequential filling occurs, as expected if one of the sites had a significantly higher adsorption energy than the other.
(2) The interaction energy between CO molecules is considered to be site independent. This approximation is more open to question and is in principle not correct because the ratio of linear to bridge intensities is coverage dependent,[10] but it is necessary to keep the model at a reasonable level of simplicity and to keep down the number of fitting parameters.

A posteriori we shall see that even with these assumptions a good fit to the data may be obtained with reasonable values of the parameters.

The procedure involves equilibration of the lattice and determination of the differential heat. First, for a chosen coverage, molecules are adsorbed on an array of lattice sites, and

then equilibration is initiated, by randomly choosing a molecule and trying to move it to a new position: The move is accepted with unit probability if the final energy is lower than the initial energy but if the energy difference ΔE is positive it is accepted with probability $\exp(-\Delta E/kT)$, following the usual Monte Carlo prescription. The procedure is repeated many times for different molecules; usually, for an 8×8 array, 400 000 steps are sufficient and the convergence of the equilibration is checked by computing the total energy which should vary smoothly with coverage. The differential energy is determined after equilibration by adsorbing further particles in a manner consistent with the Monte Carlo prescription and averaging the change in energy over all available sites. Periodic boundary conditions are included to avoid finite size effects. The choice of a small lattice (8×8) is dictated by the need for a reasonable computing time, and does not affect the features of the plot up to high coverages, at which point the values for the energy change on adsorption begin to develop significant statistical errors due to the small number of sites available. Longer simulations with larger arrays are unlikely to improve the description and the understanding of the adsorption process.

The energy corresponding to each configuration is calculated as follows.

(1) Each CO molecule is assigned an adsorption energy to the substrate, $\epsilon_0=217$ kJ $(\text{mol})^{-1}$ taken from the experimental data at a coverage of ~0.1 ML, thus avoiding the effect of defects at low coverages;
(2) two molecules on *nnn* diagonal sites are assigned a repulsive interaction ϵ_d to account for the fall in heat observed at 0.25 ML, when diagonal sites start to be filled; and
(3) a high pairwise repulsive interaction is assigned to molecules on *nn* sites, to prevent the total coverage reaching 1 ML.

The result of the simulation is shown in Fig. 4 (upper part) for $\epsilon_0=217$ kJ/mol and $\epsilon_d=5$ kJ/mol, providing a good fit to the experimental data. The value of ϵ_d is comparable to that calculated using the function given by Persson *et al.* in their Monte Carlo simulation of CO adsorption on Pt{111}.[23] As the coverage of 0.5 ML is approached, an ordered $c(2\times2)$ structure develops and the restructuring is completed when all diagonal sites have been filled, in agreement with LEED observations.

The situation on the hex surface is more complex, potentially because CO induces restructuring to the (1×1) structure. A (1×1) island growth mechanism has been proposed,[3,10,11] with high local CO coverage within the (1×1) islands and very low CO coverage on the hex surface. As a first approximation, a constant heat of adsorption would be expected in such a situation. On the hex surface the differential heat decreases by only 16 kJ/mol between $\theta=0$ and $\theta=0.5$: this behavior is consistent with an almost constant local coverage on the (1×1) islands forming during adsorption. A high local coverage is consistent with the picture suggested by Hopkinson *et al.* in their model of CO adsorption.[9,12] It is moreover consistent with a low-frequency shift for the high-frequency (linear) CO band (less than 7 cm^{-1}) compared to a 21 cm^{-1} shift on the (1×1) surface.[11] This picture also agrees with LEED observations[10] showing (1/2,1/2) spots to be 1/3 of the maximum intensity even at a total coverage of 0.2 ML on the initially hex surface while for the (1×1) initial state the same intensity is reached only when the coverage is 0.4 ML. We conclude that adsorption on the hex surface lifts the reconstruction almost immediately: Were that not true, an abrupt change in the differential heat should be observed when the lifting of reconstruction is started at some finite coverage (0.13 ML following[11]); we thus disagree with the assignment of a 2084 cm^{-1} band to adsorption on the unreconstructed hex surface[11] and suggest that this feature may be due to adsorption on defects, where we observe a higher heat of adsorption for $\theta\leqslant0.05$ ML. This assignment is consistent with the vibrational frequencies reported for CO on stepped Pt surfaces.[24]

Since no adsorption on the hex surface is detected it is possible to express the total coverage θ as the product of the local coverage θ_l and the fractional coverage of the surface by the (1×1) phase, $\theta_{1\times1}$. Disregarding the change in the local coverage, the differential heat on the hex phase, q_{diff}, may be written as

$$q_{\text{diff}}=(-q_{\text{spt}}/\theta_l)+q_{\text{int}}(\theta_l), \tag{2}$$

where q_{spt} is the energy difference between the clean hex and the (1×1) phases, previously derived as 20 kJ $(\text{mol Pt}_s)^{-1}$, and $q_{\text{int}}(\theta_l)$ is the integral heat of adsorption on the (1×1) phase. If the local coverage is assumed to be ~0.47 (Ref. 9) a value for q of about 165 kJ/mol is obtained, which is in reasonable agreement with the observed average value in the 0–0.5 ML range (Fig. 1). The disagreement at low coverage, where the experimental value is higher than expected by 15 kJ/mol, may be attributed to adsorption at defect sites. The total contribution of the adsorption at defects to the integral heat is thus estimated as about $(0.4\times15$ kJ/mol/2)/$0.5\approx6$ kJ/(mol CO), which gives an error in q_{spt} of about 3 kJ $(\text{mol Pt}_s)^{-1}$, i.e., comparable with the experimental uncertainty [2 kJ $(\text{mol Pt}_s)^{-1}$, Ref. 17].

In the range from 0.5 to 0.75 ML the (1×1) and hex surfaces exhibit the same behavior and the values of the heats of adsorption and of the sticking probabilities are the same within experimental error, as expected since at 0.5 ML the state of the two surfaces is the same (Fig. 3). It is difficult to describe in a quantitative way the rapid fall of the heat of adsorption in the range of coverage from 0.5 ML to saturation (0.75 ML) because of the complexity of the structures involved. Qualitatively however, the diminished distance between CO molecules accounts for the strong decrease in the heat of adsorption, due to intermolecular repulsions and to adsorption site changes. A change in the positions of CO molecules with increasing coverage is consistent with rapid changes in the work function, which might be explained by changes in the dipole moment of the adsorbed species.

The sticking probability measured on the hex surface is in excellent agreement with previous results by Hopkinson *et al.*[12] and by Behm.[10] Two pathways for adsorption have

been suggested:[12] The main one, which accounts for the linear decrease of s with coverage, is adsorption on the clean hex phase [followed by conversion to the (1×1) structure]; there is also an alternative and less important pathway, which accounts for the small deviation from linearity, consisting of trapping in a mobile precursor on the (1×1) islands followed by hopping to the surrounding clean hex phase for final accommodation.

The sticking probability behavior on the (1×1) surface is, however, at variance with previous work. We have carefully checked this point but always obtained reproducible results, and the difference cannot be due to the method or to the calibration because the results obtained for the hex surface are consistent. The difference must therefore be traced to the preparation procedure followed in the present work to obtain the (1×1) surface. Instead of adsorbing O_2 at high temperature, as suggested by Barteau *et al.*,[15] we sputtered the hex surface and then adsorbed O_2. The sticking coefficient on the sputtered hex surface at RT is much higher than for an annealed hex surface and at the end of the preparation procedure, which also involves hydrogen cleaning, LEED exhibited a (1×1) pattern. It is tentatively suggested that even though the surface is converted locally to a (1×1) structure by oxygen adsorption and hydrogen reduction, the long-range order is not as good as obtained with other preparation procedures. Thus, the initial sticking probability is lower. This also explains why the pronounced precursorlike behavior reported by other researchers[10,12] is not observed. As we already pointed out briefly in Sec. II of this paper, the differential heat of adsorption is expected to be unaffected by the long-range order of the surface because it is mainly determined by the formation of metal-molecule bonds and by repulsive interactions between near neighbor molecules, two parameters which do not depend on the degree of surface order.

B. NO adsorption

We discount the possibility that NO dissociation contributes significantly to the adsorption heat measurements. Although Pirug *et al.* have suggested that some dissociation takes place,[4] in a more recent paper Fink *et al.* have shown that the time scale for the surface dissociation of NO on Pt{100} at room temperature is in the region of thousands of seconds.[25] The SCAC is only responsive to processes which occur within the time scale of the adsorption pulse, i.e., 100 ms. The high initial adsorption heat (225 kJ/mol) for NO on Pt{100}(1×1), obtained at $\theta\leqslant0.05$, can therefore, as for CO, be attributed to adsorption at defect sites. It is possible that these defects are steps because the coverage at which this high heat species is saturated ($\sim$0.05 ML) corresponds to a terrace of length of about 20 atomic spacings, which is a reasonable step density for a single crystal surface. As expected, this coverage is the same as for CO adsorption, since the number of defects present on a (1×1) surface at the beginning of the experiment depends only on the preparation, which is the same for both experiments.

We now seek to explain the observed variation of adsorption heat with coverage between 0.05 and 0.15 ML on the (1×1) surface (Fig. 2), where no restructuring occurs. Two plateaus, at 200 and 180 kJ/mol, are separated by a fall at $\theta\sim0.15$ ML and followed by a fall at $0.35<\theta<0.45$. As for CO adsorption, substrate-mediated interactions between molecules play the dominant role. In introducing lateral interactions we must also account for the ordered structures observed or, as importantly, not observed. We note that (i) neither $p(2\times2)$ nor $c(2\times2)$ structures are observed; and (ii) a $c(2\times4)$ structure is observed only close to saturation. The former implies that the pairwise repulsive interaction between two molecules aligned in nnn positions along the diagonal of the lattice is higher than for two molecules in nn positions, while the latter implies that it is energetically not favorable to have a structure in which each molecule has $4nn$'s and that a structure with only $2nn$ molecules is preferred. Moreover, the absence of a $p(2\times2)$ structure also implies that some interaction between molecules causes chains to be favored. The structure suggested for the $c(2\times4)$ pattern by Gardner *et al.*[3] does not possess a glide line and is inconsistent with the observation of missing beams in the LEED pattern, but we acknowledge that chains of molecules have to be formed in order to satisfy the spectroscopic constraint of having only one kind of adsorption site. An alternative structure which fully accounts for the observed $c(2\times4)$ LEED pattern and the RAIRS data of Gardner *et al.*[3] is shown in Fig. 5(a): Nitric oxide molecules are displaced from on top positions, and a glide line is present. In order to explain the observed behavior of the differential heat it is necessary that for coverages up to 0.15 ML no substantial repulsive interactions are involved, thus explaining the constant value of the differential heat observed. At about 0.15 ML filling of sites with some molecules in nnn sites has to start, and a similar process must be completed without further substantial contributions at a coverage of 0.35 ML; at this point further and stronger repulsive interactions are invoked to explain the final drop in the heat. The values of the coverages corresponding to the two falls in the adsorption heat suggest a possible model.

The main hypothesis for our model is that a configuration of three neighboring adsorbed molecules in displaced positions [configuration T in Fig. 5(b)] has a lower repulsive interaction than (i) two neighboring molecules (configuration C in the same figure) and (ii) two next neighbors molecules, i.e., on diagonal sites (configuration D). This situation may appear unusual but it might arise as the result of a complex balancing of through-space and substrate-mediated forces between molecules. The suggestion does need backing from full quantum-mechanical calculations. The model also requires the assumption that when triplets are in nn on-line configuration to one another (configuration TT), stronger triplet–triplet pairwise repulsive interactions are invoked.

Monte Carlo simulations were performed to test the model and to obtain interaction energies by fitting to the data. The procedure applied is the same used for CO adsorption with equilibration of the lattice and determination of the differential heat. The choice of a lattice model with only one kind of adsorption site is supported by spectroscopic evi-

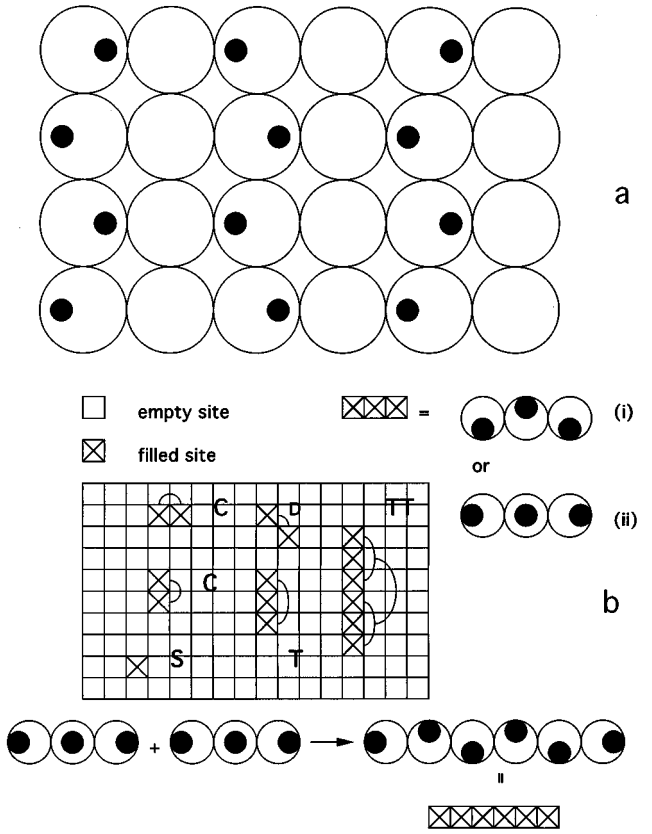

FIG. 5. (a) The structure suggested for NO on Pt{100}. Large white circles are Pt atoms and smaller black circles are NO molecules. (b) Some of the possible configurations considered in the Monte Carlo simulation are shown; their meaning is explained in the text.

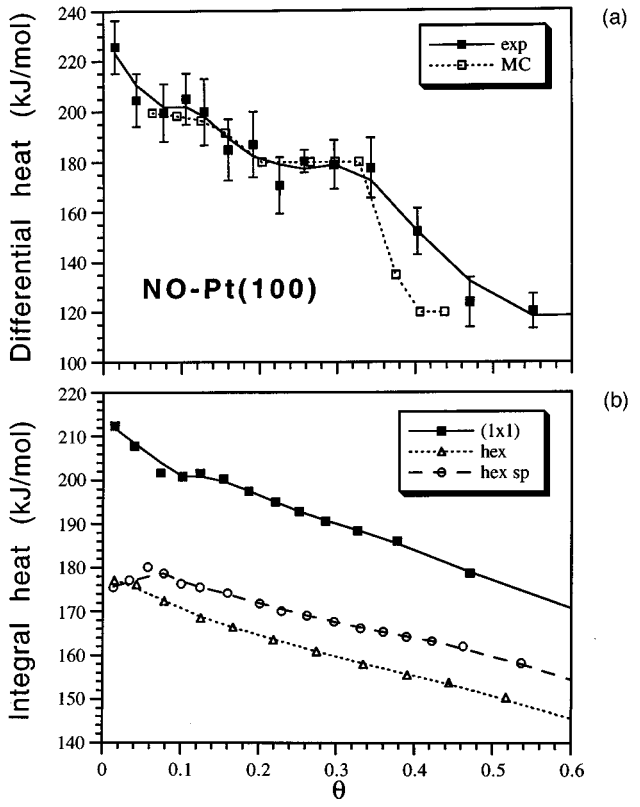

FIG. 6. (a) A comparison between Monte Carlo simulation (MC) for the coverage dependence of the differential heat of adsorption of NO on Pt{100}(1×1) and the experimental data (exp). (b) The integral heats of adsorption of NO on Pt{100} for the three initial states of the surface of Fig. 2.

dence showing only one IR band, assigned to a displaced position, intermediate between atop and bridge sites. The energy of each configuration is calculated as follows.

(a) Each NO molecule [singleton S in Fig. 5(b)] is assigned an adsorption energy to the substrate, $\epsilon_0=200$ kJ/mol, taken from the experimental data in the range of coverage around 0.1 ML.

(b) High pairwise repulsive interactions are assigned to two molecules on nn sites (C) or on diagonal sites (D) to prevent formation of a $c(2\times2)$ structure, and to prevent the total coverage exceeding 0.5.

(c) A small repulsive interaction energy ϵ_t is assigned to each triplet (T) of molecules, to generate the observed fall in the adsorption heat between 0.15 and 0.2 ML.

(d) A larger repulsive interaction ϵ_{tt} is assigned to two nn triplet pairs (TT) or to two triplets and an isolated molecule, corresponding to the completion of the rows along the glide line and accounting for the final drop in differential heat after 0.4 ML.

The result of the simulation is shown in Fig. 6 (upper part) for $\epsilon_0=200$ kJ/mol, $\epsilon_t=20$ kJ/mol, and $\epsilon_{tt}=80$ kJ/mol, providing a good fit to the experimental curve. The snapshots (shown in Fig. 7) of the structures at intermediate coverages show no ordered structures, in agreement with LEED observation. At full coverage, the structure does show strings of molecules separated by empty rows, but does not include the in-phase displacements across the strings which produce the $c(2\times4)$ structure [Fig. 5(a)]. A further interaction term is needed to incorporate this feature into the model, but here we note that energetically this is a second-order effect. The model needs confirmation of the existence of triplets at intermediate coverages. A definitive test could be provided by atomic resolution STM; published STM pictures do not show the required resolution.

Despite many attempts, we were unable to find an alternative model to account for *all* of the observed effects consistently. The drop in heat at a coverage (0.15 ML) lower than the coverage expected (0.25 ML) for a ''more conventional'' model might be ascribed to a partial ordering of the surface due to a lower mobility of the chemisorbed species, but that cannot account for the absence of a $c(2\times2)$ structure which should start to develop at a coverage close to the fall in the differential heat, as occurs with CO on the same substrate. In any case the formation of the $c(2\times4)$ structure and the absence of the $c(2\times2)$ structure, imposes stringent constraints on any model. (i) The repulsive contribution due to four neighbors [given by a $c(2\times2)$ overlayer] is higher than that given by two neighbors [as in a $c(2\times4)$], even if in this situation the separation between molecules is smaller. (ii) The most significant repulsive contributions set in only at high coverage (higher than 0.35 ML) thus implying that a

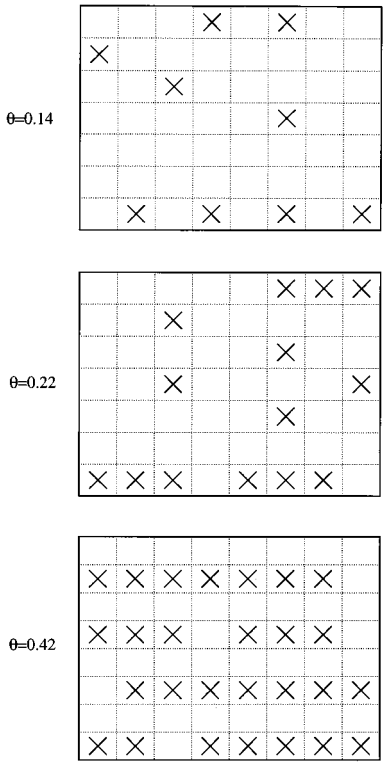

FIG. 7. Snapshots from the MC simulation at three different NO coverages on the (1×1) surface. At low coverage molecules can avoid neighbor occupancy, thus giving a heat of adsorption equal to the singleton energy. At intermediate coverage triplets or chains of molecules start to form. Finally, at high coverage, triplets join together to give the characteristic chains. If the chains are correctly interpreted, as shown in Fig. 5, a $c(2\times4)$ structure develops at high coverage, while no ordered structures form at low coverage, consistent with experimental LEED observations.

configuration must exist which allows the heat of adsorption to change only by 20 kJ/mol while the coverage increases from 0.05 to 0.35 ML.

The adsorption of NO on the hex surface may be analyzed as for CO, by using Eq. (2). Here, however, the change in the heat of adsorption in the range 0–0.45 ML, before the final drop takes place, is 38 kJ/mol, i.e., much larger than for CO adsorption, so that it is no longer correct to assume the local coverage to be constant. Using the value of q_{spt} obtained by the analysis of CO adsorption it is possible to obtain the expected differential heat by assuming the local coverage to be a function of the total coverage. However, for any reasonable choice for this function (constant, linearly increasing or even exponentially increasing) and for any reasonable value of the initial local coverage consistent with spectroscopic data (i.e., in the range from 0.3 to 0.5), we obtained an initial differential heat on the hex surface which was lower by at least 40 kJ/mol than that experimentally observed. Thus the initial heat of adsorption for NO on the hex phase is anomalously high, and we conclude that the contribution of defects to the heat of adsorption on the hex phase is much larger than on the (1×1) phase. The energetic importance of these defects is higher on the hex than on the (1×1) surface because the defects at the edges of the islands created during the reconstruction are additional to those defects initially present on the clean surface, thus causing their contribution to be significant over a wide coverage range. Accordingly on the hex surface the defect band observed in EELS[4,18] and RAIR[3] spectra increases in intensity with coverage while this band is missing on the (1×1) surface, where defect sites are saturated at a coverage as low as 0.05 ML. There is therefore a contribution due to defects which increases the initial value of the heat of adsorption and contributes about 15 kJ/mol to the integral heat at 0.5 ML, corresponding to a correction on q_{spt} of about 8 kJ $(\mathrm{mol\ Pt_s})^{-1}$. This value is much larger than the error on the evaluation of this difference [2 kJ $(\mathrm{mol\ Pt_s})^{-1}$, Ref. 17] so that we have to conclude that the final states obtained from the initial state (1×1) and hex surfaces are not the same, but energetically differ by ~7 kJ $(\mathrm{mol\ Pt_s})^{-1}$. Attributing a higher heat of adsorption to defects is consistent with results from the sputtered hex surface where the apparent value of q_{spt} [obtained by comparing the integral heats on the (1×1) and hex surfaces at the saturation coverage where the state of the surface should be the same] is even lower, and the curve for the integral heat is intermediate between the (1×1) and the ''well-prepared'' hex curves, as shown in Fig. 6. Increasing the initial surface defect density clearly gives an even larger difference between model and experiment. It has been suggested that highly defective surfaces may exhibit a stronger dissociative activity[2] which could explain the observed discrepancy between the expected differential heat and the observed one. Estimating the dissociative heat of adsorption to be around 400 to 500 kJ/mol as observed with the same calorimeter on Ni{100},[26] the maximum fraction of molecules which can dissociate in the time scale of 50 ms may be estimated to be lower than 0.1 and it does not change a lot when the surface is sputtered before adsorption.

These data show that the final states of the initially hex and (1×1) surfaces at 0.5 ML coverage of NO when starting from a (1×1) and a hex phase *are not the same*. This is confirmed by an evaluation of RAIRS,[4] UPS,[14] and LEED[1,14] data, and also supported by our observation that the sticking probability is not the same at $\theta\sim0.5$ ML for both surfaces. We note that NO is reported to partly dissociate on the (1×1) surface, while little or no dissociation is detected on the hex surface, although Sugai *et al.*[27] claim some dissociation on Pt{100}-hex; the extent of the dissociation must, however, be larger on the (1×1) surface since the Pt–O stretching mode at 560 $\mathrm{cm^{-1}}$ was observed by EELS[4,18] on the (1×1) but not on the hex surface. As already mentioned, we would not detect the heat release due to NO dissociation (estimated at around 400 to 500 kJ/mol, Ref. 26) because the time constant for NO dissociation at room temperature is $\sim10^5$ s.[25]

For all these reasons extraction of the initial state energy difference between the clean (1×1) and the hex phases from NO calorimetric data is complicated by minor effects which are difficult to estimate accurately. The CO–Pt{100} system is therefore to be preferred for the evaluation of q_{spt}.[17] A value for q_{spt} was also obtained by adsorption of ethylene which was consistent with that obtained using CO.[17] The difference in the integral heat of adsorption of NO on hex and (1×1) surfaces at saturation coverage [13 kJ

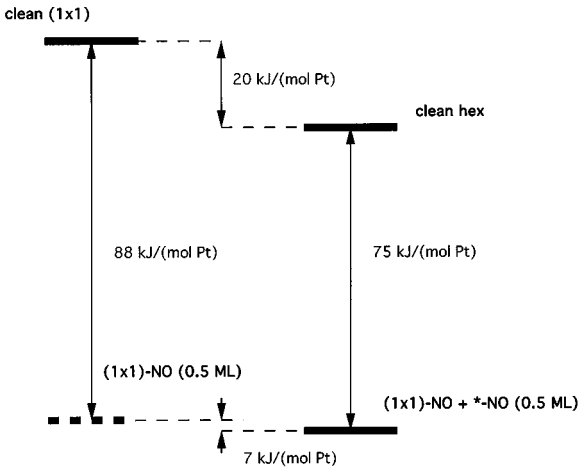

FIG. 8. Schematic energy diagram for the NO-Pt{100} system. The levels for the clean hex and the clean (1×1) surface are in the upper part of the figure. They are separated by 20 kJ $(\text{mol Pt}_s)^{-1}$, i.e., q_{spt}, as obtained from the CO data. In the lower part the energies of the final states for the initial (1×1) (left) and the initial hex (right) Pt{100} surface are shown. The final state is a (1×1) surface with coverage 0.5 ML of NO forming a $c(2\times4)$ pattern for the initial clean (1×1) (dashed line) and a (1×1) surface with coverage 0.5 ML of NO in a $c(2\times4)$ pattern plus some NO at defect sites (*) for the initial hex surface. The energy difference [7 kJ $(\text{mol Pt})^{-1}$] between the final states as obtained from the integral heats is shown.

$(\text{mol Pt}_s)^{-1}$] is just the difference in energy between the clean (1×1) and hex phases [20 kJ $(\text{mol Pt}_s)^{-1}$] *less* the energy difference between the final states [7 kJ $(\text{mol Pt}_s)^{-1}$], whatever this is caused by. Figure 8 shows a schematic energy diagram for the initial Pt{100} hex and Pt{100}(1×1) surfaces. At 0.5 ML coverage the energy of the surfaces is lowered by an amount corresponding to the integral heat multiplied by the coverage. Due to the higher adsorption heat on the (1×1) surface, the (1×1) level drops by a larger amount than the hex level, but it remains slightly higher, by an amount just equal to 7 kJ $(\text{mol Pt}_s)^{-1}$. The surface generated by NO adsorption on the initially hex phase is therefore less stable than that generated by adsorption on the initially (1×1) surface. Why, then, does the less stable state not convert to the more stable? There are two possible explanations, kinetic and thermodynamic. There may be a large activation energy barrier between the $c(2\times4)$-NO structure obtained from the (1×1) surface and the $c(2\times4)$-NO structure with defects, obtained from the hex surface. Alternatively, the true energy of the surface obtained starting from the (1×1) surface may be lower than that calculated because some slow NO dissociation occurs on the surface (as proved by EELS[4,18]): for reasonable values of the dissociative heat of adsorption of O_2 (400–500 kJ/mol) only 2% to 3% dissociation would be sufficient to remove the difference in energies. In this case, the final states reached by the initially hex and (1×1) surfaces are different due to a small degree of dissociation on the (1×1) surface.

We turn now to discuss the various interaction energies obtained for NO on Pt{100}(1×1). As indicated in Fig. 5, the linear triplet arrangement formed above $\theta=0.14$ may be either (i) an array in which the molecules are already tilted in the direction orthogonal to the row of molecules, as in the $\theta=0.5$ structure, or (ii) an array in which the central molecule is upright and the other two tilted away from it. In either case, the tilting reduces the Pauli repulsion between molecules, but the second case provides a simple explanation for the relatively large repulsive interaction energy obtained between triplet pairs; as shown in Fig. 5, this interaction leads to a rearrangement of four of the six NO molecules. Even in case (ii) we would expect a single band in RAIRS, due to dipole coupling between all three molecules in the triplet. We note that the biggest IR frequency *shift* occurs in the coverage range 0.13 to 0.25 ML,[3] where triplet formation occurs, in agreement with this model.

The sticking probability for the hex surface is initially higher than for the (1×1) surface. No precise measurements of the sticking probability as a function of coverage have been previously reported for this surface. The sticking probability on the hex surface decreases as a function of coverage almost linearly, thus demonstrating that the adsorption process is dominated by island formation. On the islands the local coverage is high so that sticking on the islands can only occur with very small probability. Only a fraction $(1-\theta/\theta_l)$ of the surface is available for adsorption, thus explaining the observed Langmuir-type behavior. The slight deviation from linearity may be explained using an argument similar to that invoked for CO by Hopkinson and King:[12] An additional adsorption pathway is present which is the impinging of NO on (1×1)-NO islands into a mobile physisorbed precursor followed by migration to the surrounding hex surface where, due to the absence of repulsive interactions, adsorption is energetically favored with conversion to the chemisorbed state. On the (1×1) surface the sticking probability is initially lower than for the hex and its decrease is linear in coverage, if the small plateau is ignored. On the (1×1) surface precursorlike behavior should be expected, by analogy with CO adsorption, but the preparation of the (1×1) surface in our work is different and properties which depend strongly on the degree of long range order of the surface may differ from other measurements.

C. Comparison between NO and CO adsorption

There are some important similarities and differences between the interaction of NO and CO with the same substrate, Pt{100}. The similarities may be summarized as follows.

(1) Both gases adsorb with high sticking probabilities on the (1×1) and hex surfaces, with zero activation barrier; the coverage dependence is similar, suggesting very similar pathways for the adsorption of CO and NO. On the hex surface the main pathway is adsorption on the clean surface followed by efficient restructuring to (1×1) islands, while on the (1×1) surface the coverage dependence is influenced by the preparation procedure which does not appear to produce a defect-free surface; this explains some disagreement with previous work on the coverage dependence of the sticking probability on the (1×1) surface.

(2) The differential heat of adsorption at low coverage is similar for both gases on both the hex and the (1×1) surfaces thus suggesting similar energetics dominated by nondissociative adsorption. On the (1×1) surface the heat of adsorption decreases with increasing coverage because of repulsive interactions between molecules while on the hex surface the restructuring to (1×1) islands with a high local coverage leads to a more gentle variation in differential heat with coverage. The higher heat of adsorption on the (1×1) surface is the driving force for the transition from the hex to the (1×1) structure.

Despite these strong similarities, there are also some intriguing and not fully understood differences in the behavior of NO and CO.

(1) The saturation coverage at 300 K is larger for CO (0.75 ML) than for NO (0.5 ML), and different overlayer structures form: at 0.5 ML a $c(2\times2)$ pattern is observed for CO adsorption while a $c(2\times4)$ structure is obtained with NO; moreover, in the range of coverage between 0.5 and 0.75 ML, CO molecules rearrange in a complex fashion forming high density structures involving loss of commensurability, unlike NO. These differences reflect the different magnitudes of repulsive interactions between adsorbed molecules; the repulsive energy associated with a triplet of NO molecules is 20 kJ/mol, corresponding to 10 kJ/mol for each pair in the triplet while for CO the repulsive energy between CO molecules on *nnn* sites is only 5 kJ/mol; when the coverage is increased it is energetically more favorable to arrange CO in a $c(2\times2)$ structure, where each molecule has four neighbors, with a total repulsive interaction of 20 kJ/mol up to 0.5 ML, while for NO it is more favorable to arrange into triplets, where each molecule has only two neighbors, thus reaching a coverage of about 0.4 ML with a total repulsive contribution of about 20 kJ/mol. To reach the coverage of 0.5 ML NO molecules have to overcome the repulsion between close triplets (80 kJ/mol) while for CO such a coverage is reached without further repulsive contributions. Thus no NO adsorption takes place beyond 0.5 ML, while CO molecules can be arranged into more complex structures to reach a saturation coverage of 0.75 ML. The detailed modeling of the heat of adsorption for NO up to 0.5 ML is complex and requires the unexpected suggestion that triplets are formed.

(2) On the (1×1) surface the role of defects is similar for NO and CO adsorption while on the hex surface the defects have a much greater influence on NO than on CO: The heat of adsorption at defect sites is higher for NO by about 25 kJ/mol, compared to a total interaction energy of about 180 kJ/mol. It is possible to attribute this difference to some NO dissociation taking place at defect sites on the hex surface, which would imply that the time constant for dissociation at defects on the hex surface is shorter than for the ''normal'' sites on the (1×1). Such a possibility is explicitly mentioned by Zemlyanov *et al.*[18] to account for a shoulder in the N_2 desorption peak which is observed on the hex but not on the (1×1) surface.

(3) CO is reported to occupy atop and bridge sites while NO occupies only one kind of adsorption site, identified as intermediate between top and bridge position on the base of vibrational frequencies. Since no sequential filling occurs on the (1×1) surface, the heat of adsorption is similar for both top and bridge sites and not very different from NO.

(4) NO dissociation does occur, particularly at higher temperatures, whereas CO does not dissociate. The heat measurements in this work confirm that on the time scale of 0.1 s the extent of dissociation at 300 K is negligible. When dissociation does take place rapidly, as for NO on Ni{100}, a considerably higher heat of adsorption, about 430 kJ/mol, has been measured by the same instrument.[26]

(5) The pre-exponential factor for desorption at high coverage is readily obtained from the sticking probability and heat measurements. In a pulsed beam experiment, at high coverages a steady state is achieved when the amount adsorbed during a 50 ms (t_1) pulse is balanced by the amount desorbed in the time ($t_2=2450$ ms) between pulses. Hence, writing the amount desorbed as $t_2\theta\nu N_s\exp[-q/(RT)]$, where q is the heat measured during the adsorption pulse, and the amount adsorbed per pulse as t_1sQ, where s is the measured sticking probability and Q is the flux, the desorption pre-exponential at the coverage θ can be determined as

$$\nu=(t_1/t_2)sQ/(\theta N_s)\exp(q/(RT)). \tag{3}$$

Here θ is the limiting coverage achieved at steady state. For CO on the (1×1) (and initially hex) surface $q\approx85$ kJ mol^{-1} at $\theta\approx0.75$ when $s\approx0.04$ (Fig. 1) with $Q=2\times10^{13}$ mol cm^{-2} s^{-1} and $N_s=1.28\times10^{15}$ atom cm^{-2}, giving $\nu\approx4\times10^{10}$ s^{-1}. For NO on the (1×1) surface, $q\approx105$ kJ mol^{-1} at $\theta\approx0.5$ when $s\approx0.1$ (Fig. 2), giving $\nu\approx4\times10^{16}$ s^{-1}. the higher value for ν compensating for the higher value for q. While the value derived for NO desorption is in the expected range, 10^{13} s^{-1} to 10^{16} s^{-1},[16] the value for CO is anomalously low, as we have recently found for CO on Pt{110}.[28]

V. CONCLUSIONS

The calorimetric heat of adsorption of NO on Pt{100} at low coverage is found to be (177 ± 6) kJ/mol on the hex surface and (200 ± 10) kJ/mol on the (1×1) surface at room temperature. The corresponding values for CO are (179 ± 3) kJ/mol and (215 ± 4) kJ/mol, respectively.

On the (1×1) surface the coverage dependence of the heats of adsorption is dominated by repulsive interactions which are particularly pronounced for NO. To explain the observed dependence and the structure forming at saturation

a model is proposed suggesting that a triplet of NO molecules is more stable than a pair in *nn* or *nnn* sites. Monte Carlo simulations provide a good fit to the data yielding the magnitude of the repulsive interactions involved, and are consistent with LEED observations. The magnitude of repulsive interactions is considerably lower for CO than for NO, which is consistent with the lower saturation coverage for NO.

On the hex surface, where islands formation occurs and the local coverage changes are limited, the heat of adsorption of CO changes by a small amount with total coverage θ, and at 0.5 ML coverage the curves for the initially hex and the (1×1) surfaces match. By comparing the integral heat of adsorption at $\theta=0.5$ from the two initial states, (1×1) and hex, the energy difference between the clean hex and (1×1) phase is obtained as 20 kJ (mol $Pt_s)^{-1}$. For NO the energetics of the hex surface is probably more influenced by adsorption at defect sites, where eventually some dissociation may take place.

Finally, comparing the results for NO and CO, it appears that the gross features (magnitudes of the heats of adsorption, sticking probabilities and adsorption kinetics) are similar while detailed properties (repulsive interactions, contributions of adsorption at defect sites to the energetics of the system, nature of the overlayer structures formed at high coverage and value of the saturation coverage) are distinctive.

ACKNOWLEDGMENTS

We thank J. Chevallier for supplying and mounting the platinum single crystal films. Adrian Wander, Alex Pasteur, Georg Held, Jo Bradley, and Manuel Perez-Jigato are acknowledged for stimulating discussions and suggestions. L.V. acknowledges ''Fondazione Angelo della Riccia'' for a Fellowship; Trinity College, Cambridge, is acknowledged for a studentship for Y.Y.Y. The U.K. EPSRC is acknowledged for an equipment grant.

[1] K. Mase and Y. Murata, Surf. Sci. **242**, 132 (1991); **277**, 97 (1992).
[2] R. J. Gorte and L. D. Schmidt, Surf. Sci. **109**, 367 (1981).
[3] P. Gardner, M. Tüshaus, R. Martin, and A. M. Bradshaw, Surf. Sci. **240**, 112 (1990).
[4] G. Pirug, H. P. Bonzel, H. Hopster, and H. Ibach, J. Chem. Phys. **71**, 593 (1979).
[5] E. Ritter, R. J. Behm, G. Pötschke, and J. Wintterlin, Surf. Sci. **181**, 403 (1987). W. Hosler, E. Ritter and R. J. Behm, Ber Bansenges. Phys. Chem. **90**, 208 (1986).
[6] St. J. Dixon-Warren, A. Pasteur, and D. A. King, J. Chem Phys. (in press).
[7] A. T. Pasteur, St. J. Dixon-Warren, and D. A. King, J. Chem Phys. (in press).
[8] H. Miki, T. Nagase, K. Sato, H. Watanabe, S. Sugai, K. Kawasaki, and T. Kioka, Surf. Sci. **287**, 448 (1993).
[9] A. Hopkinson and D. A. King, Chem. Phys. **177**, 433 (1993).
[10] R. J. Behm, P. A. Thiel, P. R. Norton, and G. Ertl, J. Chem. Phys. **78**, 7437, 7448 (1983).
[11] R. Martin, P. Gardner, and A. M. Bradshaw, Surf. Sci. (in press).
[12] A. Hopkinson, X. C. Guo, J. M. Bradley, and D. A. King, J. Chem. Phys. **99**, (1993); A. Hopkinson, J. M. Bradley, X. C. Guo, and D. A. King, Phys. Rev. Lett. **71**, 1597 (1993).
[13] P. A. Thiel, R. J. Behm, P. R. Norton, and G. Ertl, J. Chem. Phys. **78**, 7448 (1983).
[14] H. P. Bonzel, G. Brodén, and G. Pirug, J. Catalysis **53**, 96 (1978).
[15] M. A. Barteau, E. I. Ko, and R. J. Madix, Surf. Sci. **102**, 99 (1981).
[16] M. Gruyters, T. Ali, and D. A. King, Chem. Phys. Lett. **232**, 1 (1995).
[17] Y. Y. Yeo, C. Wartnaby, and D. A. King, Science **268**, 1731 (1995).
[18] D. Y. Zemlyanov, M. Y. Smirnov, V. V. Gorodetskii, and J. H. Block, Surf. Sci. **329**, 61 (1995).
[19] C. E. Borroni-Bird and D. A. King, Rev. Sci. Instrum. **62**, 2177 (1991).
[20] A. Stuck, C. E. Wartnaby, Y. Y. Yeo, J. T. Stuckless, N. Al-Sarraf, and D. A. King (submitted).
[21] D. A. King and M. G. Wells, Surf. Sci. **29**, 454 (1972).
[22] T. B. Grimley, Proc. Phys. Soc. (London) **90**, 751 (1967); **92**, 776 (1967); T. B. Grimley and S. M. Walker, Surf. Sci. **14**, 395 (1969); T. L. Einstein and J. R. Schrieffer, Phys. Rev. B **7**, 3629 (1973).
[23] B. N. J. Persson, M. Tüshaus, and A. M. Bradshaw, J. Chem. Phys. **92**, 5034 (1990).
[24] V. K. Agrawal and M. Trenary, Surf. Sci. **259**, 116 (1991); B. E. Hayden, K. Kretzschmar, A. M. Bradshaw, and R. G. Greenler, *ibid*. **149**, 394 (1985); R. G. Greenler, K. D. Burch, K. Kretzschamar, R. Klauser, A. M. Bradshaw, and B. E. Hayden, *ibid*. **152**, 338 (1985).
[25] T. Fink, J. P. Dath, M. R. Bassett, R. Imbihl, and G. Ertl, Surf. Sci. **245**, 96 (1991).
[26] L. Vattuone, Y. Y. Yeo, and D. A. King (in preparation).
[27] S. Sugai, K. Takeuchi, T. Ban, K. Miki, K. Kawasaki, and T. Kioka, Surf. Sci. **282**, 67 (1993).
[28] C. E. Wartnaby, Y. Y. Yeo, and D. A. King (in preparation).